New Phytologist

Research

Methods

An inducible CRISPR-Kill system for temporally controlled cell type-specific cell ablation in *Arabidopsis thaliana*

Fabienne Gehrke[1], Paola Ruiz-Duarte[2], Angelina Schindele[1], Sebastian Wolf[2,3] and Holger Puchta[1]

[1]Joseph Gottlieb Kölreuter Institute for Plant Sciences (JKIP) – Molecular Biology, Karlsruhe Institute of Technology (KIT), Karlsruhe, 76131, Germany; [2]Centre for Organismal Studies (COS), Ruprecht-Karls-University Heidelberg, 69120, Heidelberg, Germany; [3]Centre for Plant Molecular Biology (ZMBP), Plant Biochemistry, Eberhard-Karls-University Tübingen, 72076, Tübingen, Germany

Authors for correspondence:
Holger Puchta
Email: holger.puchta@kit.edu

Sebastian Wolf
Email: sebastian.wolf@zmbp.uni-tuebingen.de

Received: *27 January 2023*
Accepted: *25 May 2023*

New Phytologist (2023)
doi: 10.1111/nph.19102

Key words: CRISPR/Cas, development, genome editing, genome elimination, genome engineering, meristem, tissue engineering.

Summary

- The application of the CRISPR/Cas system as a biotechnological tool for genome editing has revolutionized plant biology. Recently, the repertoire was expanded by CRISPR-Kill, enabling CRISPR/Cas-mediated tissue engineering through genome elimination by tissue-specific expression.
- Using the Cas9 nuclease from *Staphylococcus aureus* (SaCas9), CRISPR-Kill relies on the induction of multiple double-strand breaks (DSBs) in conserved repetitive genome regions, such as the rDNA, causing cell death of the targeted cells. Here, we show that in addition to spatial control by tissue-specific expression, temporal control of CRISPR-mediated cell death is feasible in *Arabidopsis thaliana*.
- We established a chemically inducible tissue-specific CRISPR-Kill system that allows the simultaneous detection of targeted cells by fluorescence markers. As proof of concept, we were able to eliminate lateral roots and ablate root stem cells. Moreover, using a multi-tissue promoter, we induced targeted cell death at defined time points in different organs at select developmental stages.
- Thus, using this system makes it possible to gain new insights into the developmental plasticity of certain cell types. In addition to enabling tissue engineering in plants, our system provides an invaluable tool to study the response of developing plant tissue to cell elimination through positional signaling and cell-to-cell communication.

Introduction

Targeted cell ablation enables the analysis of cell populations in an organotypic functional context in which various questions of developmental biology can be answered, that is, cell differentiation, organ generation, and regeneration or cell-to-cell signaling *in vivo*. Additionally, for plant breeding, induction of cell ablation can be of great interest to induce female or male sterility or to trigger the ablation of select organs. Therefore, various tools for specific cell elimination have been established and further developed over the last decades (Day & Irish, 1997; Machin *et al.*, 2019; Glowa *et al.*, 2021). Besides the phototoxic induction of cell death through laser ablation (Colombelli *et al.*, 2004; Marhavý *et al.*, 2016), genetic approaches for tissue-specific cell elimination have been established. While most genetic cell ablation approaches are based on the tissue-specific expression of bacterial toxins (Goldman *et al.*, 1994; Day *et al.*, 1995; Weijers *et al.*, 2003), the application of the CRISPR/Cas system as a programmable site-specific nuclease (Jinek *et al.*, 2012) has recently enabled another method for tissue-specific cell elimination in Arabidopsis. The CRISPR-Kill system relies on massive double-strand break (DSB) induction in functional repetitive regions of DNA, namely the 45S ribosomal DNA (rDNA) tandem repeats or centromeric satellites (Schindele *et al.*, 2022). Targeting the internal transcribed spacer 2 (ITS2) of up to 750 45S rDNA tandem repeats per haploid genome resulted in a strong lethal effect when expressing the *Staphylococcus aureus* Cas9 (SaCas9) nuclease (Steinert *et al.*, 2015) constitutively (Schindele *et al.*, 2022). Moreover, localized effects such as prevention of organogenesis could be achieved by using tissue-specific promoters. In addition to spatial control, temporal control of the CRISPR-Kill system would be highly desirable to induce cell death, especially in tissues formed at early developmental stages. This would be of great added value for answering development-related questions and adding temporal flexibility to the applications of cell or organ ablation. We have previously used the GR-LhG4/pOp-mediated transactivation system (Moore *et al.*, 1998; Craft *et al.*, 2005; Samalova *et al.*, 2005) to establish a comprehensive repertoire of

transgenic Arabidopsis lines enabling spatially and temporally controlled gene expression (Schürholz *et al.*, 2018). In this setup, a driver line (Fig. 1a) is used to define the target tissue for inducible gene expression. A tissue-specific promoter limits the expression of the chimeric transcription factor GR-LhG4 in the target cells. The addition of the inducer dexamethasone (Dex) results in the translocation of the transcription factor to the nucleus where it binds to its cognate promoter, consisting of six 52 bp *lac* operator (Op6) copies in front of a cauliflower mosaic virus 35S minimal promoter, enabling tunable expression of the downstream gene based on inducer concentration. To monitor tissue specificity, the driver line encodes the reporter gene *mTurquoise2* under the control of the pOp6 promoter. The driver lines can easily be combined with different effector lines (Fig. 1b), carrying an effector gene under the control of the inducible promoter. This results in the expression line (Fig. 1c), in which the tissue-specific gene expression of the reporter and the effector can be induced. Depending on the used driver line, inducible as well as tissue-specific gene expression can be initiated in different tissues of the root apical meristem (RAM), shoot apical meristem (SAM), or vascular cambium (Schürholz *et al.*, 2018). Here, we show that the combination of the Dex-inducible system with the CRISPR-Kill approach in a tissue-specific setting enables cell ablation of very early organs in plant development, such as meristematic tissues, without the peril of lethality.

Materials and Methods

T-DNA constructs

Previously established pUbi-SaCas9-ITS2 and pUbi-SaCas9-ADH1 (Schindele *et al.*, 2022) were used as the source DNA to generate the inducible CRISPR-Kill as well as the ADH1 control construct. An *Eco*RI restriction enzyme digestion enabled the removal of PcUbi4-2. The pOp6 promoter was synthesized (BioCat GmbH, Heidelberg, Germany) and amplified (pOp6_fw 5′-TATGACATGATTACGAATTCATGCATATGTCGAGCTCAAGA-3′; and pOp6_rv 5′-TCTTCATGGCGCGCCGAATTCCGTCCTCTCCAAATGAAATGA-3′). Using Gibson Assembly® (New England Biolabs GmbH, Frankfurt am Main, Germany), the amplified pOp6 was integrated into the EcoRI-digested constructs, resulting in the expression vectors pOp6:SaCas9-ADH1 as well as pOp6:SaCas9-ITS2. The pAHP6 promoter was amplified from Arabidopsis pAHP6>>4-1_#668 genomic DNA (pAHP6_fw 5′-TATGACATGATTACGAATTCACGGGGCGCAAAGAAGCATG-3′ and pAHP6_rv 5′-CTTCATGGCGCGCCGAATTCCAACGGCACACCCGTCTTGT-3′) integrated into the *Eco*RI-digested constructs using Gibson Assembly®, resulting in the expression vectors pAHP6-SaCas9-ADH1 as well as pAHP6-SaCas9-ITS2. For the generation of the proof-of-concept pUbi-GR-LhG4 construct, the coding sequence of GR-LhG4 was amplified from *Arabidopsis thaliana* (L.) Heynh. pXPP>>D10-2001 genomic DNA (GR-LhG4_fw 5′-TGCAGCGAATTCGGCGCGCCATGGCTAGTGAAGCTC-3′ and GR-LhG4_rv 5′-GGCCTGGAGCTCGGCGCGCCTTACTCTTTTTTTGGGTTTG-3′). Using Gibson Assembly®, the amplified GR-LhG4 was integrated into a *Asc*I-digestion linearized pUbi-tPea3A vector resulting in the pUbi-GR-LhG4-tPea3A construct. Final constructs were confirmed by Sanger sequencing in *Escherichia coli* using the software ApE for alignment and analysis of the sequence data. Correct T-DNA constructs were integrated into *A. thaliana* via *Agrobacterium*-mediated transformation via floral dip. For the determination of sgRNA expression, total RNA was extracted from pools of 14-d-old seedlings for each line. Subsequently, 1 µg RNA was applied for cDNA synthesis using the qScript® cDNA Synthesis Kit (Quantabio, Beverly, MA, USA). For quantitative real-time PCR, 1 µl of cDNA, 5 µl of 2× qPCR Master Mix KAPA SYBR FAST (Sigma-Aldrich Chemie GmbH), 0.5 µl forward and reverse primer (10 mM, P1-P5, Supporting Information Table S1) were combined and filled up with distilled water to a total volume of 10 µl. The Light Cycler480 instrument (384-well block system; Roche Diagnostics) was used for analysis. All single-locus lines and the reference gene *ACTIN2* were tested in three technical replicates. Source data are provided as Table S1.

Plant material and growth conditions

Experiments were performed in the *A. thaliana* background Columbia (Col-0). Plants were either cultivated in the glasshouse on soil (1 : 1 mixture of Floraton (Floragard Vertriebs-GmbH, Oldenburg, Germany) and vermiculite (2–3 mm; Deutsche Vermiculite Dämmstoff, Sprockhövel, Germany)) or under sterile conditions in CLU-36L4 plant culture chambers (Percival Scientific, Perry, IA, USA) in long-day settings (16 h : 8 h, light : dark) at 22°C. After sterilization with 4% sodium hypochlorite and stratification overnight at 4°C, seeds were grown on germination

Fig. 1 Setup of the inducible CRISPR-Kill system in *Arabidopsis thaliana*. (a) The driver line of the inducible, tissue-specific CRISPR-Kill harbors two elements. A tissue-specific promoter (pTS) that controls the expression of a chimeric transcription factor (GR-LhG4) and a fluorescent reporter (mTurquoise2) that stains the target tissue after induction, controlled by an inducible promoter (pOp6-TATA). (b) The effector line also carries two elements, the SaCas9 nuclease under the expression of the pOp6-TATA promoter and the respective guide RNA (gRNA) which is constitutively expressed via the U6-26 promotor. (c) Combination of the driver line with the effector line results in the expression line. Adding the inducer dexamethasone (Dex) externally at a desired time point, Dex binds to GR-LhG4 and activates the expression of the fluorescence reporter marking the target tissue. At the same time, the DNA break induction is activated, resulting in cell death of the target cell. (d) Determination of relative survival after culturing the inducible expression lines for 3 wk on 0, 50, or 100 µM Dex-containing selection medium. While Dex treatment of the ADH1 control lines showed no significant (ns) differences in the number of surviving plants compared to the approach without Dex-induction, only 12% (50 µM) and 7% (100 µM) survived in the CRISPR-Kill lines (internal transcribed spacer 2, ITS2) compared to the approach without Dex-induction. Data are shown as normalized mean values ± SD and the statistical difference was calculated using the two-tailed *t*-test with unequal variances: ***, $P < 0.001$; $n = 3$ biologically independent experiments. (e) Representative images of the ADH1 control as well as the CRISPR-Kill lines (ITS2). To induce plant cell death at a later time point, 26-d-old plants were transferred to medium containing 100 µM Dex. After 21 d, the plants were phenotypically analyzed. While the CRISPR-Kill lines died, the control plants continued to grow normally.

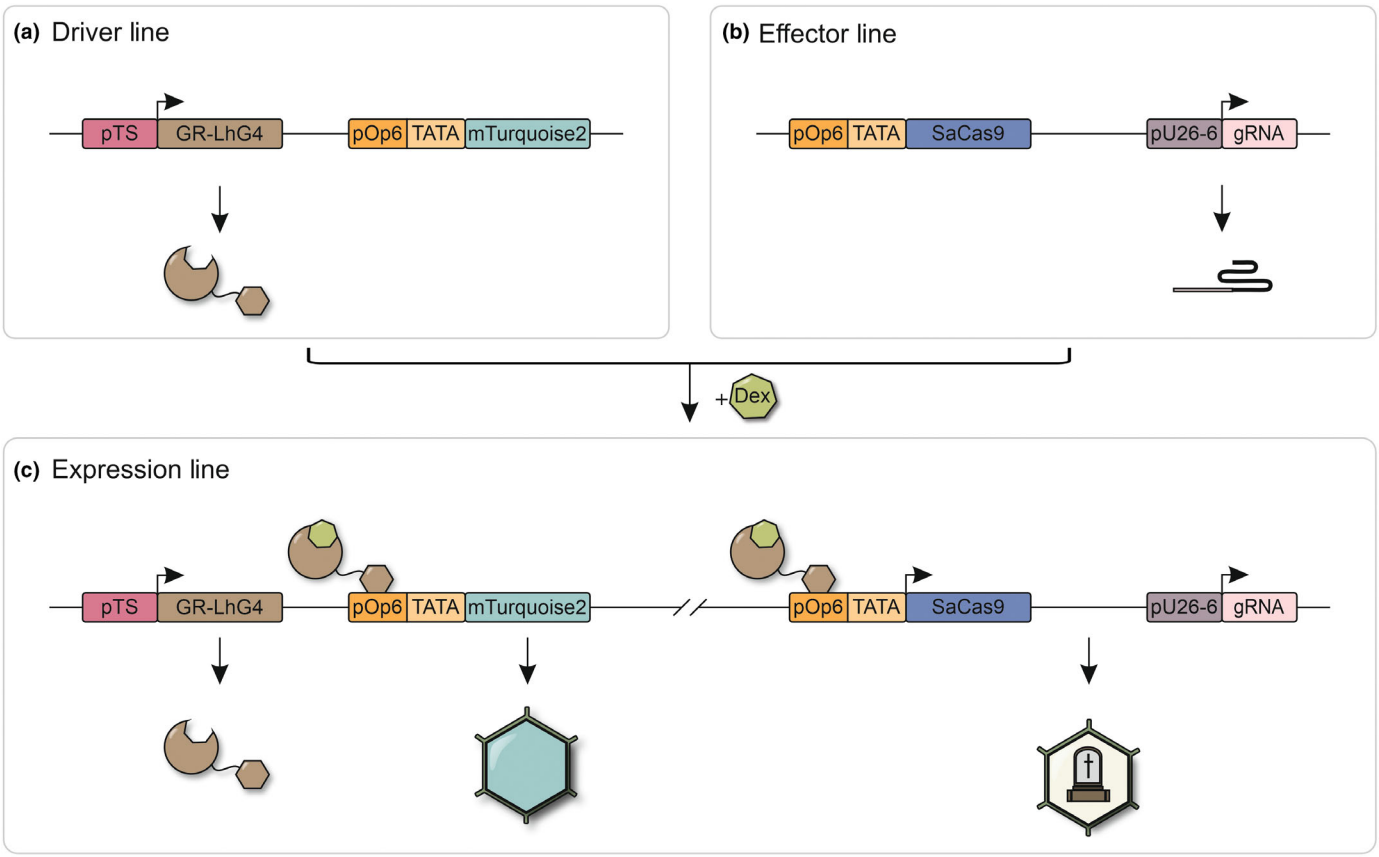

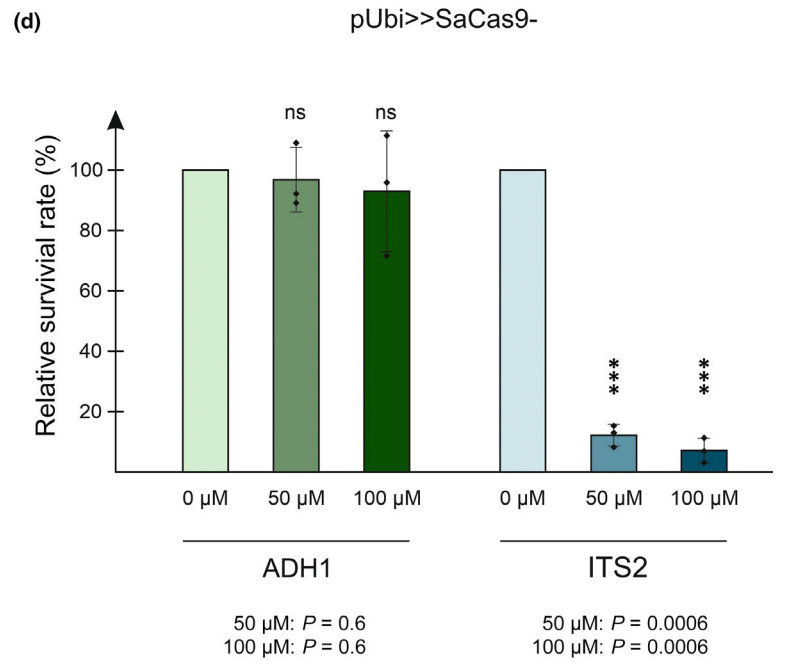

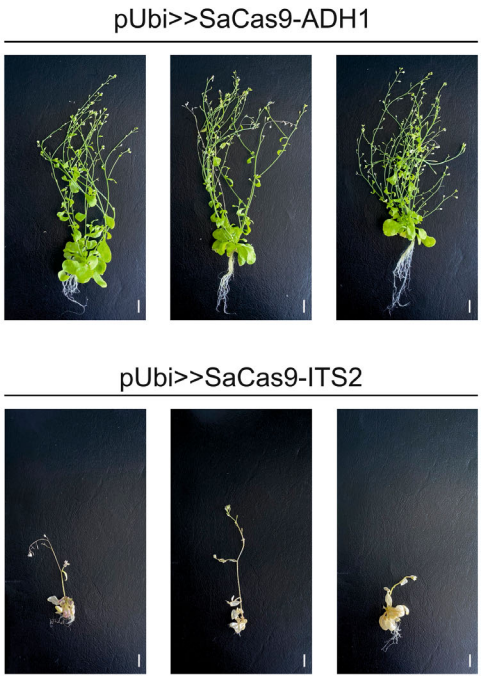

medium (GM: 4.9 g l^{-1} Murashige & Skoog medium (Duchefa), 10 g l^{-1} Suc, and 8 g l^{-1} Agar; pH 5.7 with potassium hydroxide), whereas agar concentration was raised to 10 g l^{-1} for root analyses on vertical plates. For the establishment of the expression lines, driver lines pAHP6>>4-1_#668, pXPP>>D10-2001, or pSCR>>17-0215_#680 (Schürholz *et al.*, 2018) were crossed as a maternal parent with the effector lines pOp6:SaCas9-ADH1 or pOp6:SaCas9-ITS2 as a paternal parent. F1 seeds were selected

on medium with 3.75 μg ml^{-1} sulfadiazine for the driver line construct and 6 μg ml^{-1} DL-Phosphinotricin (PPT) or 60 μg ml^{-1} gentamicin for the effector line construct. For induction of gene expression, plants were sown on/or transferred to plates containing Dex (D4903; Sigma-Aldrich) resolved in DMSO at the indicated concentrations.

Determination of T1 survival rate

To determine the relative survival rate, T1 seeds were sown on herbicide- (and inducer-) containing medium. After 3 wk, the total number of seeds and the number of transgenic plants were counted and set into relation. We defined a plant as viable when it passed the four leaves stadium and showed no developmental deficiency. Source data are provided as Tables S2 and S3.

Phenotypic analysis

To analyze CRISPR-Kill-mediated cell death in pUbi-positive cells in later developmental stages, transgenic plants were selected on herbicide-containing medium for 2 wk in three independent technical replicates. After another 12 d of growth in cultivation boxes, the plants were transferred to cultivation boxes with 100 μM Dex or an equal amount of DMSO. The Phenotypic evaluation was performed after another 21 d. For the analysis of roots, F2 seeds were spread on vertical root plates containing herbicide (and Dex) within the indicated concentrations. In total, 80 plants, divided into three technical replicates out of two independent T-DNA insertion lines, were transferred to Dex- or DMSO-containing plates 5 d after germination and phenotypically analyzed after another 10 d of growth. Besides counting the lateral root number, the primary root length was determined by the ImageJ add-on SmartRoot (Lobet *et al.*, 2011). Source data and box plots of the independent T-DNA lines are provided as Tables S4–S6 and Figs S1–S3.

Microscopy

Root samples were imaged using a Zeiss LSM 700 laser scanning microscope with a Zeiss Plan-Apochromat ×63/1.4 oil-immersion objective. The mTurquoise2 fluorophore was excited at 405 nm, and emission was collected between 460 and 550 nm. To visualize dead cells and the cell walls of living cells, samples were stained with 5 μg ml^{-1} PI (P4170; Sigma-Aldrich) and imaged with 555 nm for excitation, and emission was collected between 566 and 630 nm. SAM imaging was performed as described (Schürholz *et al.*, 2018).

Statistical methods

Differences in survival rates were determined by applying a two-sided, two-sample *t*-test with unequal variance. For root number and primary root length, a one-way ANOVA was performed: ns, $P > 0.05$; *, $P \leq 0.05$; **, $P < 0.01$; ***, $P < 0.001$; ****, $P < 0.0001$.

Results

Establishment of the inducible CRISPR-Kill system

To provide an inducible context for the CRISPR-Kill system, the toolkit for inducible and tissue-specific gene expression, established by Schürholz *et al.* (2018) in *Arabidopsis,* was used. For the establishment of effector lines, we used the CRISPR-Kill construct SaCas9-ITS2 and, as a control, the construct SaCas9-ADH1, which is designed to induce only a unique DSB in the *ADH1* gene (Schindele *et al.*, 2022). To allow temporal control of SaCas9 expression, the nuclease was placed under the control of pOp6 and a minimal cauliflower mosaic virus 35S promoter, while the gRNA was expressed constitutively (Fig. 1b). The corresponding T-DNAs, pOp6:SaCas9-ITS2 and pOp6:SaCas9-ADH1, were transformed in *A. thaliana* Columbia-0 (Col-0) background via *Agrobacterium*-mediated transformation. After selection and propagation of the primary transformants, single-locus T2 lines were analyzed for their gRNA expression level in a quantitative real-time PCR to identify lines likely to enable efficient DSB induction. For both approaches, pOp6:SaCas9-ADH1 and pOp6:SaCas9-ITS2, two independent T-DNA insertions lines, were selected and propagated to homozygosity. As a proof of concept, we decided to test GR-LhG4 expression under the control of the parsley *UBI* (ubiquitin) promoter that allows the expression of transgenes in buds, roots, stems, flowers, and seeds in *A. thaliana* (Plesch & Ebneth, 2011). Therefore, we transformed an expression vector harboring *GR-LhG4* under the control of the *UBI* promoter into homozygous pOp6:SaCas9-ITS2 plants as well as into the control line, pOp6:SaCas9-ADH1. To induce CRISPR-Kill activity, primary transformant selection was performed on herbicide medium containing 50 or 100 μM Dex. As a control experiment, seeds of the same batch were selected on a medium without Dex. While the control lines showed a similar survival rate in all three conditions, a significant decrease in the number of transgenic plants containing the pUbi-driven inducible pOp6:SaCas9-ITS2 constructs was observed in correlation with increasing inducer concentration. Compared with the DMSO control, a reduction of survival rate by 88% could be observed when plants were grown on 50 μM Dex and by 93% on 100 μM Dex (Fig. 1d). These data are in line with the results of the constitutive system (Schindele *et al.*, 2022) and suggest that cell death can be efficiently induced through the GR-LhG4 system. To test whether similar effects can be achieved at a later stage of plant development, 26-d-old primary transformants were transferred to a medium containing 100 μM Dex or DMSO. After another 21 d of growth, in 37% of transgenic plants, death of the entire plant was observed, characterized by developmental arrest after Dex induction (Fig. 1e). These results strongly suggest that CRISPR-Kill-mediated cell death can be efficiently induced with the Dex-based system in a temporally controlled manner.

Inducible CRISPR-Kill-mediated organ ablation

As we were successful in the induction of whole-plant cell death by constitutive expression of the Dex-binding transcription

factor, we were further interested in whether cell death could be restricted to a specific tissue or organ by selecting a tissue-specific promoter instead. In the RAM, the *XPP* promoter (At4g30450, Andersen *et al.*, 2018) is active in the xylem pole pericycle (XPP) cells containing the lateral root founder cells, which show some characteristics of dormant stem cells. Since pXPP had already been successfully used in the constitutive tissue-specific CRISPR-Kill system to ablate lateral roots (Schindele *et al.*, 2022), we were curious whether the use of this XPP-specific promoter (Fig. 2a) in the Dex-induced approach could cause similar phenotypes. Therefore, we crossed the pXPP driver line with the previously established homozygous effector lines, pOp6:SaCas9-ITS2 and pOp6:SaCas9-ADH1. The respective expression lines were grown on medium containing DMSO, 50 or 100 μM Dex and the lateral root number was determined (Fig. 2b,c). As expected, the control lines showed no significant reduction in lateral root number with increasing inducer concentration. By contrast, in the CRISPR-Kill lines, culturing the plants on 50 μM inducer halved the number of lateral roots compared with the approach without Dex-induction. Moreover, further reduction could be achieved by adding 100 μM Dex, resulting in a threefold reduction in the lateral root amount compared to the approach without Dex. No lateral roots were formed in one-third of the evaluated plants, demonstrating the remarkable efficiency of this approach. Despite the drastic reduction in lateral root number, the CRISPR-Kill lines showed sustained growth of the main root (Fig. 2d). To visualize the induced CRISPR-Kill effect at the cellular level, expression of the *pOp6*-controlled *mTurquoise2* reporter was examined by confocal laser scanning microscopy 12 h after Dex induction in 4-d-old seedlings. Roots were counterstained with the fluorescent dye propidium iodide (PI), which visualizes cell outlines and enters dead cells labeling DNA in the nucleus, serving as a viability stain. While the fluorescent signal of the mTurquoise2 reporter could be detected in the target tissue in all analyzed lines, the CRISPR-Kill lines additionally showed dead cells exclusively in the pXPP cells, confirming the highly cell-specific nature of this approach (Fig. 2e).

Inducible cell ablation in the root apical meristem

We next tested whether the inducible CRISPR-Kill system is also feasible for the ablation of stem cells at a defined time point. Therefore, we chose the pSCR driver line using the promoter of the GRAS family transcription factor *SCARECROW* (*SCR*; At3g54220, Di Laurenzio *et al.*, 1996; Wysocka-Diller *et al.*, 2000), which is active in the QC and endodermis as well as the cortex/endodermis initials of the RAM. The root stem cell niche consists of the infrequently dividing cells of the quiescent center (QC), which are surrounded by initials, mitotically active stem cells. The division of the different initials results in a predictably ordered tissue organization of the root (Dolan *et al.*, 1993). SCR plays an essential role in the specification and maintenance of the QC as well as formative divisions of the ground tissue initials, which give rise to cortex and endodermis cells (Di Laurenzio *et al.*, 1996; Sabatini *et al.*, 2003; Cui *et al.*, 2007). A new QC is also formed during the establishment of the lateral root meristem. During the *de novo* formation of lateral root QC, SCR expression is necessary for controlling the formative periclinal cell divisions of the outer layer of stage II lateral root primordia from which QC precursor cells are formed (Goh *et al.*, 2016). Therefore, we were interested in whether pSCR-dependent CRISPR-Kill activity would have an impact on lateral root formation. To generate the respective expression lines, homozygous pOp6:SaCas9-ITS2 as well as pOp6:SaCas9-ADH1 lines were crossed with the pSCR driver line. For lateral root number analysis, we transferred 5-d-old seedlings of the corresponding expression lines to medium containing 50 or 100 μM Dex. After 10 d of induction, no significant change was observed in the ADH1 control lines with increasing inducer concentration, whereas the induced CRISPR-Kill lines showed a dramatic reduction in lateral root number (Fig. 3a). Uninduced plants grown on DMSO without Dex developed on average 7.5 lateral roots per plant, whereas plants grown on Dex were almost devoid of lateral roots. Compared with the DMSO control without Dex, the induced CRISPR-Kill plants displayed a relative lateral root number of 3.5% (50 μM) and 2.7% (100 μM). This suggests that loss of pSCR-positive cells prevents lateral root formation. Since cell division of cortex and endodermal cell layers is genetically activated via the SCR/SHORT ROOT (SHR) pathway (Sozzani *et al.*, 2010; Cruz-Ramírez *et al.*, 2012), and shortened root length has already been demonstrated in *scr-1* mutant experiments (Wysocka-Diller *et al.*, 2000; Sharma *et al.*, 2022), we were interested to see whether this phenotype also occurs in our CRISPR-Kill lines. Indeed, the induced CRISPR-Kill plants exhibited a significant 2.5-fold reduction in main root length (Fig. 3b) indicating that the loss of pSCR-positive cells retards primary root growth. To follow the changes in the stem cell niche of the primary root, 4-d-old roots were transferred to media containing 100 μM Dex and analyzed microscopically after different time points of induction. Already after 12 h of induction, the first dead cells could be observed in the area of the QC and young endodermis cells, while the signal of the simultaneously expressed reporter marked the target tissue (Fig. 3c). After 24 h of Dex treatment, a strong signal of the cell death marker was observed in QC, initials, and young endodermis cells of the apical meristem, whereas fluorescence of the reporter could be detected only sporadically, indicating extensive tissue elimination. The cellular consequences were observed after 48 h of induction. Here, fluorescence signals of both markers were detected only in a few spots in the area of initial cells. Also, the mTurquoise2 and the PI signal were restricted to a narrow strip next to the cortex. First periclinal cell divisions were noticeable in the adjacent inner cell layer (Fig. 3d) suggesting that the pericycle cells re-enter the cell cycle, forming pericycle daughter cells that re-differentiate into new endodermal cells. Furthermore, after 72 h of induction, a remarkable disruption of the oriented cell division patterns was observed. In contrast to the ordered tissue organization in the ADH1 control lines (Fig. 3e), formative cell divisions and re-establishment of reporter expression in ectopic positions were detected (Fig. 3d). This highly distinct phenotype is reminiscent of what has been observed after laser ablation of cells in the root ground tissue

New Phytologist

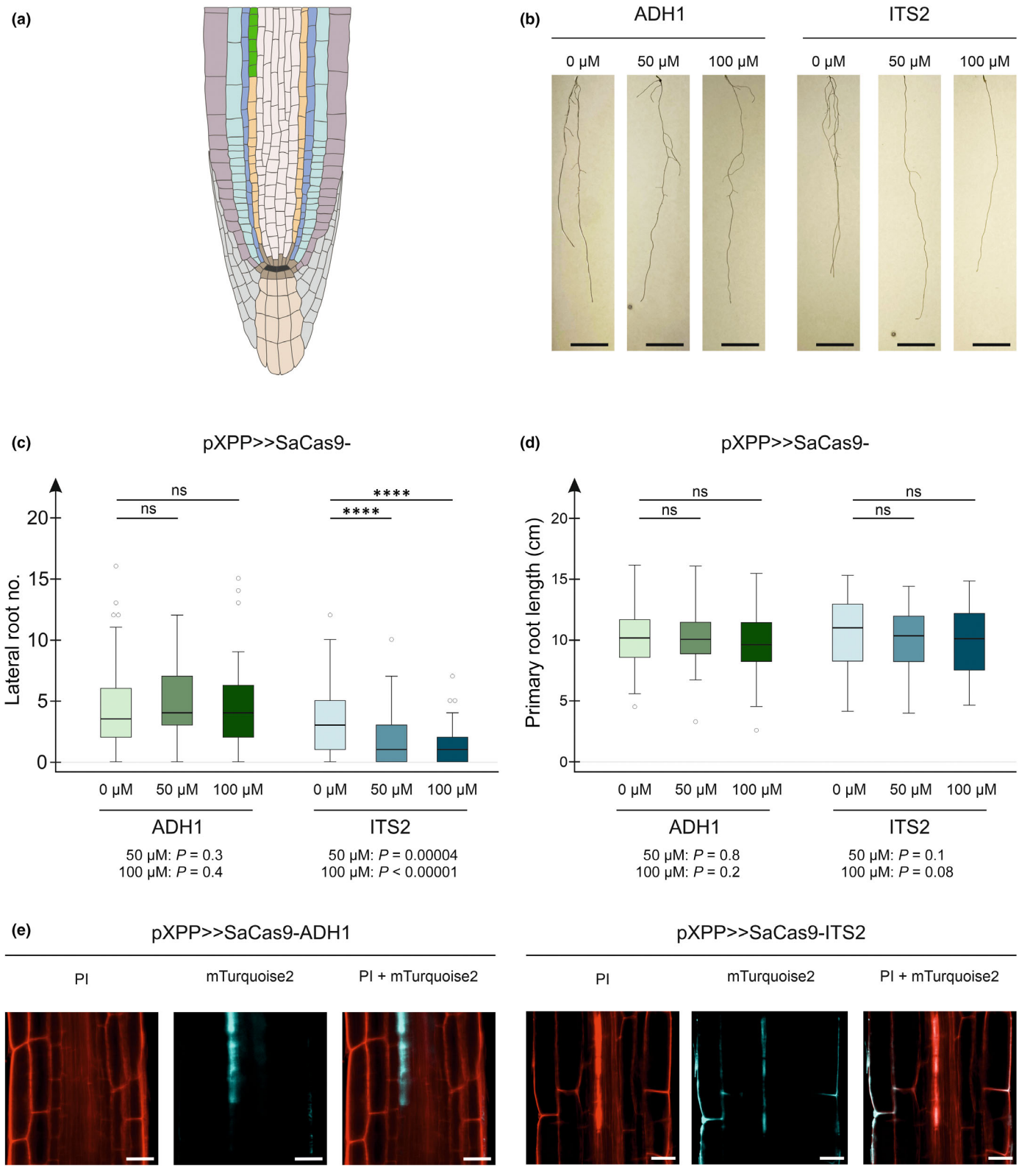

(Marhava *et al.*, 2019; Hoermayer *et al.*, 2020) and confirms the efficiency and specificity of the inducible CRISPR-Kill approach in root stem cells and further opens up new opportunities to study questions related to developmental biology.

Cell elimination in root and shoot meristems

To test the CRISPR-Kill system in a more complex context, we next chose the promoter of *HISTIDINE PHOSPHOTRANSFER*

Fig. 2 Dex-induced CRISPR-Kill activity for lateral root elimination in *Arabidopsis thaliana*. (a) Schematic representation of root tissue layer with pXPP-active cells (green). In the center of the lateral root cap (grey) lies the quiescent center (QC, black) which is surrounded by initials cells (dark brown). These form the columella (beige), epidermis (purple), cortex (light blue), endodermis (dark blue), pericycle (yellow), and stele (white). (b) Representative pictures of lateral roots of the ADH1 control lines as well as the CRISPR-Kill lines (internal transcribed spacer 2, ITS2) on different dexamethasone (Dex) concentrations (0 μM/50 μM/100 μM). Bars, 1 cm. (c, d) Phenotypic evaluation of the induced CRISPR-Kill-mediated cell death in roots. Total number of lateral roots (c) in control lines (ADH1) and CRISPR-Kill lines (ITS2) which were cultivated on different concentrations of the inductor Dex. While the control lines showed no significant change in relative root number compared to the approach without Dex (0 μM), the CRISPR-Kill lines exhibited a twofold (50 μM) and a threefold decrease (100 μM) in relative root number compared to the approach without Dex (0 μM). Analysis of the primary root length (d) showed that the control lines, as well as the CRISPR-Kill lines, displayed no significant (ns) difference compared to the approach without Dex. Data are shown in box plots ($n = 80$ out of three technical replicates), boxes indicate the first to third quartile with median, whiskers comprise 1.5× the interquartile range reaching the minimum and maximum, whereby data beyond that threshold are indicated as outliers. *P*-values were calculated using the one-way ANOVA test: ****, $P < 0.0001$. (e) Representative microscopy images of the ADH1 control lines and the CRISPR-Kill lines in which expression of the mTurquoise2 reporter as well as the SaCas9 nuclease was induced for 12 h on 100 μM Dex 4 d after germination in the xylem pole pericycle (XPP) cells. The induced lines displayed fluorescence of the mTurquoise2 reporter (green) as well as that of the propidium iodide (PI)-stained (red) cell walls of living cells and the cell volume of dead cells, respectively. Bars, 20 μm.

PROTEIN6 (*AHP6*; At1g80100). AHP6 is involved in the root specification of protoxylem cell identity and in the formation of lateral roots (Mähönen *et al.*, 2006; Moreira *et al.*, 2013). Besides its activity in RAM protoxylem precursor and pericycle cells, AHP6 is also involved in the regulation of phyllotactic patterns and is expressed during organ initiation and development in SAM. As *pAHP6* is active in organ founder cells in the shoot (Besnard *et al.*, 2014), we sought to investigate the consequences of a constitutive approach by expressing SaCas9 nuclease directly under the control of this promoter. Therefore, we transformed Col-0 plants with pAHP6-SaCas9-ITS2 and, as a control, with pAHP6-SaCas9-ADH1 constructs and determined the relative survival rate. Compared with the control, a dramatic decrease in transformants was observed for the pAHP6:CRISPR-Kill construct, leading to a relative survival rate of only 2.2% compared with the control construct (Fig. 4a). In the following, the same promotor was tested for the inducible CRISPR-Kill system. We crossed the pOp6:SaCas9-ITS2 and pOp6:SaCas9-ADH1 lines with the respective pAPH6 driver line (Schürholz *et al.*, 2018). Inducible CRISPR-Kill lines germinated on Dex-containing medium showed malformed (true) leaf primordia and failed to develop normally, whereas control lines were unaffected (Fig. 4b). However, in contrast to constitutive expression, seedling survival was not impaired. Although differences in expression strength cannot be ruled out, this might suggest that lethality due to constitutive expression from the *AHP6* promoter occurs in the embryo. To detect tissue-specific induction of cell death in the cells that give rise to leaves and flowers through formative cell divisions, SaCas9 nuclease expression was induced after 5 wk of growth. Inflorescence meristems of 15-cm-tall plants were treated with 10 μM Dex or only the solvent DMSO as control. After 96 and 120 h of induction, the inflorescence meristems were dissected and microscopically analyzed for cell viability with PI (Fig. 4d). CRISPR-Kill induction in pAHP6-positve cells led to an accumulation of internal PI fluorescence with remarkable efficiency. The massive cell death in organ primordia was consistent with the macroscopic phenotype of severely deformed and fused inflorescence meristems (Fig. 4c).

To investigate the CRISPR-Kill effect in RAM, we transferred F2 plants to medium with different Dex concentrations 5 d after germination and determined the lateral root number (Fig. 5a) as well as the primary root length (Fig. 5b) after 10 d of tissue-specific SaCas9 expression. Whereas the length of the primary root remained unaffected, a significant reduction in lateral root number, to 65% (100 μM Dex), was observed in the ITS2 cleavage lines compared to the approach without Dex-induction (0 μM Dex). The ADH1 control lines showed no significant change in lateral root number and primary root length with increasing inducer concentration. Since pAHP6 enables the inducible expression of the CRISPR-Kill system in the pericycle where lateral root formation begins, these results were in line with our expectations. Moreover, we were able to detect cell death in the pericycle of CRISPR-Kill lines at the microscopic level. Thus, we could show a coincidence of the fluorescence signal of the target tissue-labeling mTurquoise2 reporter and the PI-internalizing dead cells. In comparison with the ADH1 control lines (Fig. 5c), the fluorescence signal of the reporter was interrupted, whereby gaps were filled by the PI signal of dead cells. In addition, we observed periclinal cell divisions in adjacent cells, followed by the re-establishment of reporter expression in ectopic positions (Fig. 5d). This suggests that neighboring cells, including those of endodermal origin, are triggered to re-enter the cell cycle to compensate the loss of pericycle cells. These findings demonstrate that a multi-tissue promoter can be used to enable tissue-specific expression of the CRISPR-Kill system and thereby induce targeted cell death at defined time points. This provides a novel opportunity to gain fundamental insights into the stability and adaptation of meristems.

Discussion

In this study, we successfully combined the Dex-inducible GR-LhG4/pOp system with the novel tissue engineering tool CRISPR-Kill (Schindele *et al.*, 2022), enabling spatially and temporally controlled cell ablation in Arabidopsis. Based on a comprehensive set of driver lines (Schürholz *et al.*, 2018), we were able to fluorescently label the target tissue while simultaneously inducing tissue-specific expression of the SaCas9 nuclease. Ensuing DSB induction in the ITS2 of rDNA tandem repeats led to the death of different cell types of the shoot and root apical meristem and interrupted organogenesis of the affected cell type. We confirmed the validity of our approach via various analytical

New Phytologist

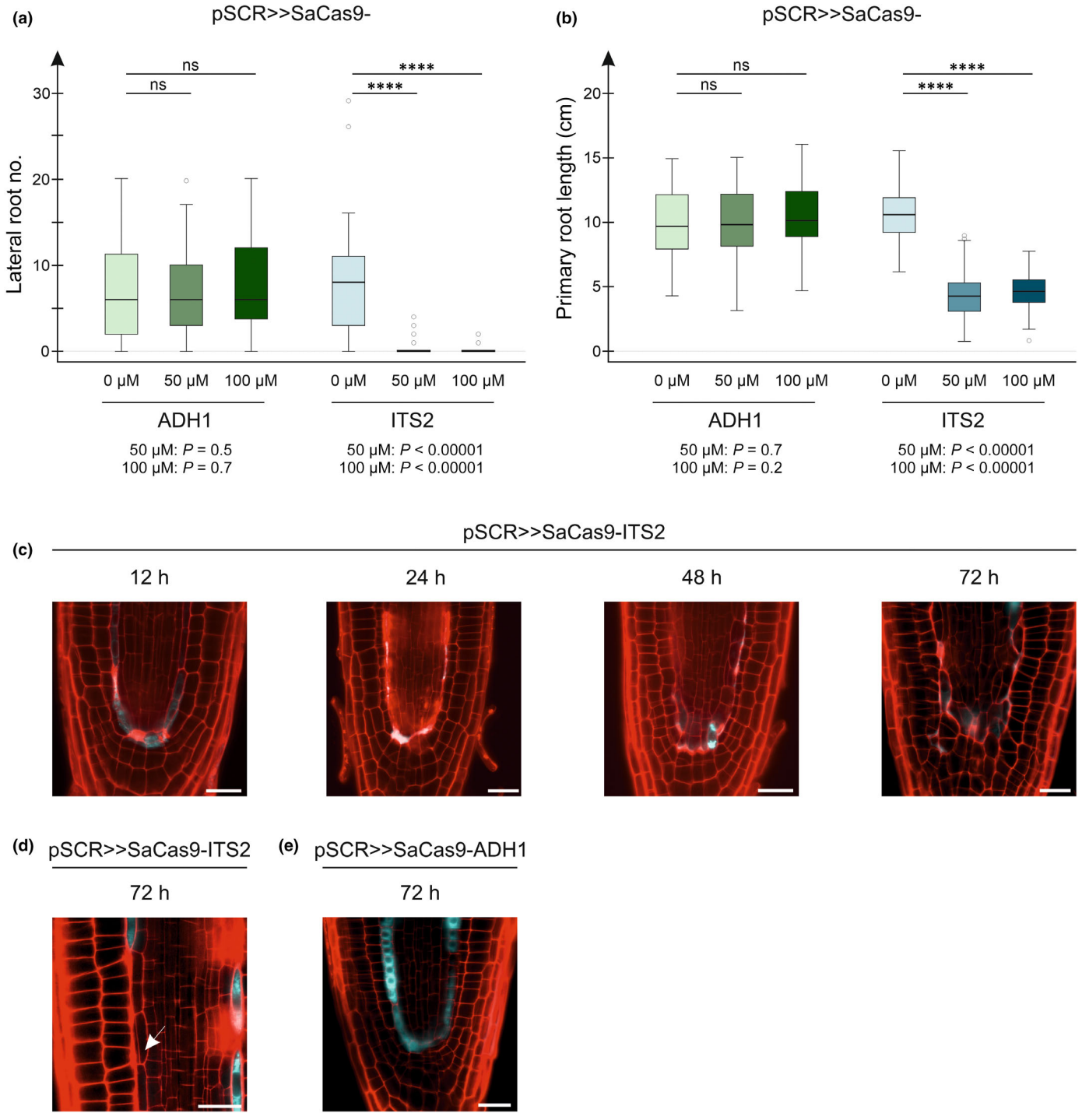

Fig. 3 Inducible CRISPR-Kill system for root stem cell ablation in *Arabidopsis thaliana*. (a, b) Phenotypic evaluation of the induced CRISPR-Kill-mediated cell death in root stem cells. Total number of lateral roots (a) of the control lines (ADH1) and the CRISPR-Kill lines (internal transcribed spacer 2, ITS2) which were cultivated using different concentrations of the inductor dexamethasone (Dex). The control lines showed no significant (ns) change in root number compared to the approach without Dex-induction. By contrast, the CRISPR-Kill lines exhibited an average of 0.3 (50 µM) and 0.2 (100 µM) lateral roots per plant compared to the approach without Dex (7.5 lateral roots; 0 µM). Also, analysis of the primary root length (b) showed that the control lines (ADH1) displayed no significant (ns) difference compared to the approach without Dex-induction, whereas the CRISPR-Kill lines (ITS2) exhibited on average a 2.5-fold shortened primary root. Data are shown in box plots ($n = 80$ out of three technical replicates), boxes indicate the first to third quartile with median, whiskers comprise 1.5× the interquartile range reaching the minimum and maximum, whereby data beyond that threshold are indicated as outliers. *P*-values were calculated using the one-way ANOVA test: ****, $P < 0.0001$. (c–e) Representative microscopy images of pSCR-positive cells in RAM. PI (red) was used to counterstain living cells as well as an indicator of dead cells. Simultaneously to the induction of the SaCas9 nuclease, the fluorescent reporter mTurquoise2 (green) was expressed, marking the tissue to be eliminated. Next to cell death in endodermal pSCR-positive cells of root basal meristem, expression of the CRISPR-Kill system resulted in severe deformations in the RAM stem cell region with increasing induction duration (c) and formative cell division in adjacent cell layers (d). The ADH1 control lines showed no change in ordered tissue organization (e). Arrows indicate formative cell division. Bars, 20 µm.

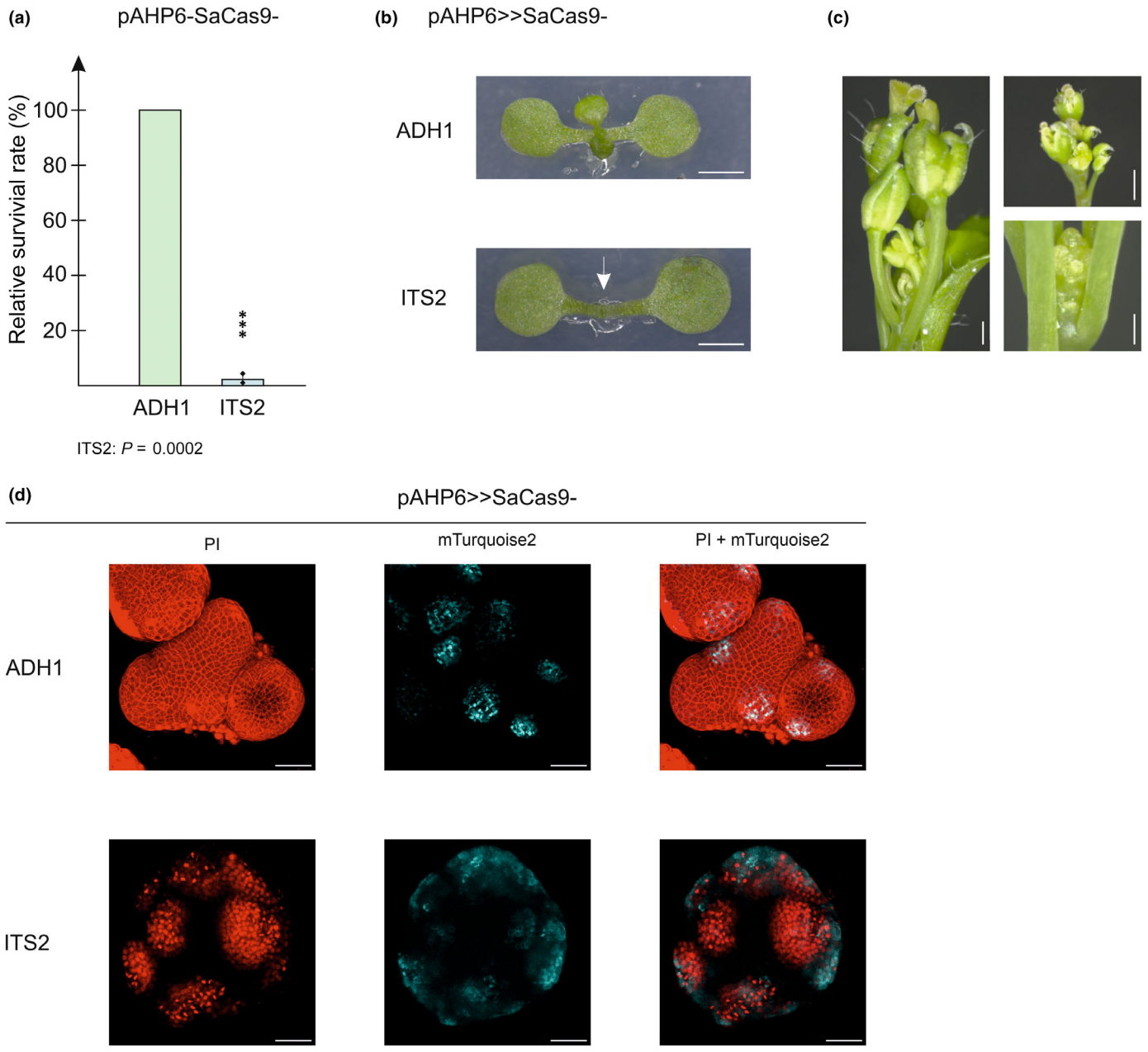

Fig. 4 Dex-induced CRISPR-Kill system with a multi-tissue promotor in the shoot apical meristem (SAM) of *Arabidopsis thaliana*. (a) Transformation of Col-0 plants with pAHP6-SaCas9-ITS2 (internal transcribed spacer 2) resulted in a reduction of the survival rate by 98% compared to the pAHP6-SaCas9-ADH1 control lines ($n = 3$ biologically independent experiments). Data are shown as normalized mean values ± SD and the statistical difference was calculated using the two-tailed *t*-test with unequal variances: ***, $P < 0.001$. (b) To determine whether the reduced relative survival was due to the expression of the CRISPR-Kill system in SAM, seedlings were transferred to inductor-containing medium. While the ADH1 control lines formed the first true leaves, the induction of cell death in the organ primordia of the CRISPR-Kill lines led to the termination of the meristem (arrows). Bars, 2 mm. (c) Representative images of the deformed inflorescence meristem after induction of the CRISPR-Kill system in SAM organ primordia. Bars, 1 cm. (d) Representative microscopy images of pAHP6-positive cells in organ primordia in SAM of the ADH1 control lines and CRISPR-Kill lines after 120 h. Propidium iodide (PI) (red) was used to counterstain living cells as well as an indicator of dead cells. Simultaneously to the induction of the SaCas9 nuclease, the fluorescent reporter mTurquoise2 (green) was expressed, marking the tissue to be eliminated. Bars, 30 μM.

methods and demonstrated the remarkable efficacy of the inducible and cell-type-specific CRISPR-Kill system. As a proof of concept, we demonstrated that the inducible CRISPR-Kill system with the constitutive Ubiquitin promoter led to plant death in early, but also later developmental stages. Moreover, we succeeded in circumventing the lethal effect when using the multi-tissue promoter pAHP6 in a constitutive tissue-specific CRISPR-Kill system. We are now able to induce cell death in root and shoot at well-defined time points and analyze local effects in RAM and SAM almost independently of each other. In addition, we were able to gain first insights into interesting possibilities for future analyses from a developmental biology perspective using

New Phytologist

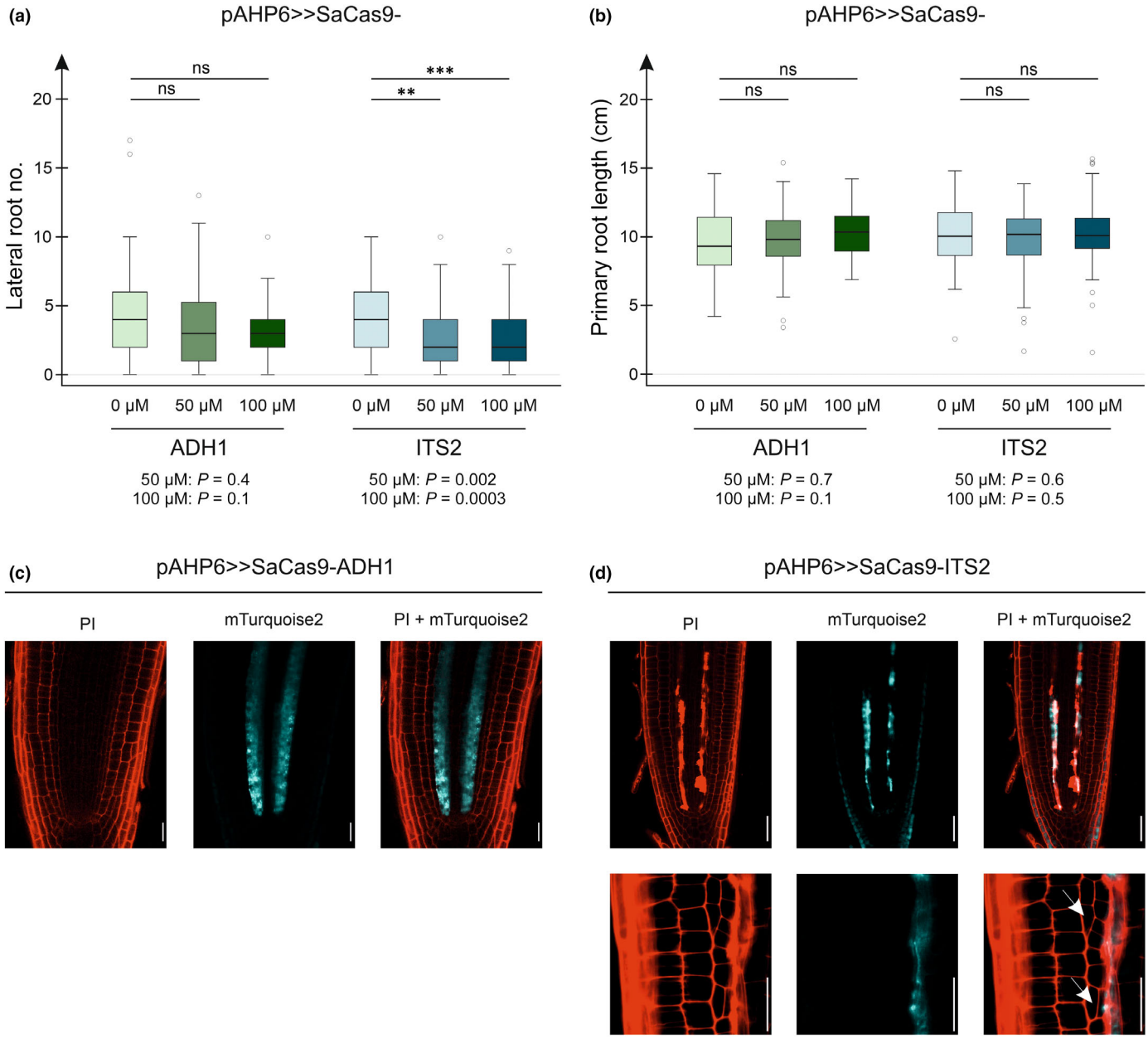

Fig. 5 Dex-induced CRISPR-Kill system with a multi-tissue promotor in the RAM of *Arabidopsis thaliana*. (a, b) Phenotypic evaluation of the induced CRISPR-Kill-mediated cell death in roots. Total number of lateral roots (a) in control lines (ADH1) and CRISPR-Kill lines (internal transcribed spacer 2, ITS2) which were cultivated on different concentrations of the inductor dexamethasone (Dex) for 10 d starting at 5 d after germination. While the induced control lines showed no significant reduction (ns) compared to the approach without Dex-induction (0 µM), the CRISPR-Kill lines exhibited a relative root number of 63% (50 µM) and 66% (100 µM) compared to the approach without Dex (0 µM). Analysis of the primary root length (b) showed that the control lines, as well as the CRISPR-Kill lines, displayed no significant (ns) difference compared to the approach without Dex-induction. Data are shown in box plots ($n = 80$ out of three technical replicates), boxes indicate the first to third quartile with median, whiskers comprise 1.5× the interquartile range reaching the minimum and maximum, whereby data beyond that threshold are indicated as outliers. *P*-values were calculated using the one-way ANOVA test: **, $P < 0.01$; ***, $P < 0.001$. (c, d) Representative microscopy image of the ADH1 control lines and the CRISPR-Kill lines in which expression of the mTurquoise2 reporter as well as the CRISPR-Kill system was induced for 24 h on 100 µM Dex 4 d after germination in pAHP6-positive cells. The induced lines displayed fluorescence of the mTurquoise2 reporter (green) as well as that of the propidium iodide (PI)-stained (red) dead cells as well as cell walls of living cells, respectively. Ectopic cell division is marked with arrows. Bars, 20 µm.

the CRISPR-Kill system in an inducible and tissue-specific context. Thus, we observed the response to the loss of pSCR-positive meristematic cells at various time points, which resulted in pronounced ectopic cell division of the QC adjacent tissue and, beyond the initials, in formative cell division of the inner-lying pericycle cells. The capability to initiate cell division for rebuilding the different injured tissues has already been demonstrated in several UV laser ablation experiments targeting the young lateral root cap, epidermis, cortex, or endodermis (Marhavý *et al.*, 2016; Marhava *et al.*, 2019). Here, ablation of up to three cells resulted

in a switch from anticlinal to periclinal cell division of exclusively the inner adjacent tissue layer and restoration of the injured cells, although this ability diminished with increasing distance from the QC (Marhava *et al.*, 2019). Interestingly, in our approach, the elimination of pAHP6-positive pericycle cells also resulted in ectopic cell division of the endodermis, which in this case is the outer cell layer, suggesting that this tissue can restore not only the cortex but also pericycle cells. To understand the underlying signaling cascades for restorative patterning, our inducible CRISPR-Kill lines may provide an attractive method to elucidate the consequences of wound response. Thereby, the established inducible CRISPR-Kill effector lines can be easily combined with a comprehensive set of existing or new driver lines to address a wide variety of questions. The analysis of the cellular consequences after cell ablation in the SAM could be of particular interest. Since these cells are often difficult to reach by laser, an inducible CRISPR-Kill approach may provide information on stem cell maintenance. Inducible CRISPR-Kill provides a precise and easily controllable alternative to previous time-definable techniques. Mostly, mechanical ablation approaches of single, easily accessible cells by UV laser treatment are pursued; however, inducible genetic approaches have also been established in recent years. These are based on the chemically inducible and tissue-specific expression of the bacterial Diphtheria toxin A (DT-A), which induces cell death by inhibiting translation and has already been used in various developmental biology studies (Day & Irish, 1997; Tsugeki & Fedoroff, 1999; Laplaze *et al.*, 2005). Thus, tissue-specific expression of DT-A in GLABRA2-positive cells was used to test the regulation and specificity of the estradiol-inducible XVE system in the atrichoblast file of the epidermis. Interestingly, neither a clear cell death phenotype nor a reporter signal could be detected in RAM, which was reasoned to be due to the translation-inhibitory effect of the DT-A toxin (Machin *et al.*, 2019). In another approach, tissue-specific expression of DT-A was induced with Dex in the GR-LhG4/pOp system to investigate functional information of the AP2/ERF transcription factor DORNRÖSCHEN-LIKE (DRNL) in founder cells of leaves and floral organs by analyzing the phenotypic consequences of cell ablation (Glowa *et al.*, 2021). Since our approach does not directly interfere with the protein biosynthesis of the reporter, the CRISPR-Kill system is a valid and useful alternative. For studies that require a reliable reporter signal, that is, for characterizations of re-differentiation after ectopic cell divisions, the addition of a second marker gene might be worth considering to further improve this system. Taken together, we expect the inducible CRISPR-Kill system to serve as an invaluable tool to study positional signaling and cell type establishment in the native tissue context with unprecedented spatial and temporal specificity.

Acknowledgements

The authors thank Maike Edler and Giulia Keller for excellent technical assistance, Michelle Roenspies for critical reading of the manuscript, and the Heidelberg Karlsruhe Strategic Partnership (HEiKA) for funding (Funding period 2020). Research in the Wolf Laboratory was furthermore supported by the German Research Foundation (DFG) with grants WO 1660/2-2 and WO 1660/6-2. Open Access funding enabled and organized by Projekt DEAL.

Competing interests

None declared.

Author contributions

HP, SW, AS and FG conceived the research. FG and SW designed the research. FG and PR-D conducted the research. FG, AS, SW, and HP wrote the paper.

ORCID

Fabienne Gehrke https://orcid.org/0000-0002-6749-9315
Holger Puchta https://orcid.org/0000-0003-1073-8546
Paola Ruiz-Duarte https://orcid.org/0000-0001-5912-0080
Sebastian Wolf https://orcid.org/0000-0003-0832-6315

Data availability

The datasets generated and analysed during this study are provided as Supporting Information. Driver lines and the majority of plasmids are already available at NASC and Addgene, respectively (Schürholz *et al.*, 2018).

References

Andersen TG, Naseer S, Ursache R, Wybouw B, Smet W, De Rybel B, Vermeer JEM, Geldner N. 2018. Diffusible repression of cytokinin signalling produces endodermal symmetry and passage cells. *Nature* **555**: 529–533.

Besnard F, Refahi Y, Morin V, Marteaux B, Brunoud G, Chambrier P, Rozier F, Mirabet V, Legrand J, Lainé S *et al.* 2014. Cytokinin signalling inhibitory fields provide robustness to phyllotaxis. *Nature* **505**: 417–421.

Colombelli J, Grill SW, Stelzer EHK. 2004. Ultraviolet diffraction limited nanosurgery of live biological tissues. *Review of Scientific Instruments* **75**: 472–478.

Craft J, Samalova M, Baroux C, Townley H, Martinez A, Jepson I, Tsiantis M, Moore I. 2005. New pOp/LhG4 vectors for stringent glucocorticoid-dependent transgene expression in Arabidopsis. *The Plant Journal* **41**: 899–918.

Cruz-Ramírez A, Díaz-Triviño S, Blilou I, Grieneisen VA, Sozzani R, Zamioudis C, Miskolczi P, Nieuwland J, Benjamins R, Dhonukshe P *et al.* 2012. A bistable circuit involving SCARECROW-RETINOBLASTOMA integrates cues to inform asymmetric stem cell division. *Cell* **150**: 1002–1015.

Cui H, Levesque MP, Vernoux T, Jung JW, Paquette AJ, Gallagher KL, Wang JY, Blilou I, Scheres B, Benfey PN. 2007. An evolutionarily conserved mechanism delimiting SHR movement defines a single layer of endodermis in plants. *Science* **316**: 421–425.

Day C, Irish V. 1997. Cell ablation and the analysis of plant development. *Trends in Plant Science* **2**: 106–111.

Day CD, Galgoci BF, Irish VF. 1995. Genetic ablation of petal and stamen primordia to elucidate cell interactions during floral development. *Development* **121**: 2887–2895.

Di Laurenzio L, Wysocka-Diller J, Malamy JE, Pysh L, Helariutta Y, Freshour G, Hahn MG, Feldmann KA, Benfey PN. 1996. The SCARECROW gene regulates an asymmetric cell division that is essential for generating the radial organization of the Arabidopsis root. *Cell* **86**: 423–433.

Dolan L, Janmaat K, Willemsen V, Linstead P, Poethig S, Roberts K, Scheres B. 1993. Cellular organisation of the *Arabidopsis thaliana* root. *Development* **119**: 71–84.

Glowa D, Comelli P, Chandler JW, Werr W. 2021. Clonal sector analysis and cell ablation confirm a function for DORNROESCHEN-LIKE in founder cells and the vasculature in Arabidopsis. *Planta* **253**: 27.

Goh T, Toyokura K, Wells DM, Swarup K, Yamamoto M, Mimura T, Weijers D, Fukaki H, Laplaze L, Bennett MJ *et al.* 2016. Quiescent center initiation in the Arabidopsis lateral root primordia is dependent on the SCARECROW transcription factor. *Development* **143**: 3363–3371.

Goldman MH, Goldberg RB, Mariani C. 1994. Female sterile tobacco plants are produced by stigma-specific cell ablation. *EMBO Journal* **13**: 2976–2984.

Hoermayer L, Montesinos JC, Marhava P, Benková E, Yoshida S, Friml J. 2020. Wounding-induced changes in cellular pressure and localized auxin signalling spatially coordinate restorative divisions in roots. *Proceedings of the National Academy of Sciences, USA* **117**: 15322–15331.

Jinek M, Chylinski K, Fonfara I, Hauer M, Doudna JA, Charpentier E. 2012. A programmable dual-RNA-guided DNA endonuclease in adaptive bacterial immunity. *Science* **337**: 816–821.

Laplaze L, Parizot B, Baker A, Ricaud L, Martinière A, Auguy F, Franche C, Nussaume L, Bogusz D, Haseloff J. 2005. GAL4-GFP enhancer trap lines for genetic manipulation of lateral root development in *Arabidopsis thaliana*. *Journal of Experimental Botany* **56**: 2433–2442.

Lobet G, Pagès L, Draye X. 2011. A novel image-analysis toolbox enabling quantitative analysis of root system architecture. *Plant Physiology* **157**: 29–39.

Machin FQ, Beckers M, Tian X, Fairnie A, Cheng T, Scheible W-R, Doerner P. 2019. Inducible reporter/driver lines for the Arabidopsis root with intrinsic reporting of activity state. *The Plant Journal* **98**: 153–164.

Mähönen AP, Bishopp A, Higuchi M, Nieminen KM, Kinoshita K, Törmäkangas K, Ikeda Y, Oka A, Kakimoto T, Helariutta Y. 2006. Cytokinin signaling and its inhibitor AHP6 regulate cell fate during vascular development. *Science* **311**: 94–98.

Marhava P, Hoermayer L, Yoshida S, Marhavý P, Benková E, Friml J. 2019. Re-activation of stem cell pathways for pattern restoration in plant wound healing. *Cell* **177**: 957–969.

Marhavý P, Montesinos JC, Abuzeineh A, van Damme D, Vermeer JEM, Duclercq J, Rakusová H, Nováková P, Friml J, Geldner N *et al.* 2016. Targeted cell elimination reveals an auxin-guided biphasic mode of lateral root initiation. *Genes & Development* **30**: 471–483.

Moore I, Gälweiler L, Grosskopf D, Schell J, Palme K. 1998. A transcription activation system for regulated gene expression in transgenic plants. *Proceedings of the National Academy of Sciences, USA* **95**: 376–381.

Moreira S, Bishopp A, Carvalho H, Campilho A. 2013. AHP6 inhibits cytokinin signaling to regulate the orientation of pericycle cell division during lateral root initiation. *PLoS ONE* **8**: e56370.

Plesch G, Ebneth M. 2011. *Method for the stable expression of nucleic acids in transgenic plants, controlled by a parsley-ubiquitin promoter.* U.S. Patent 8030539B2.

Sabatini S, Heidstra R, Wildwater M, Scheres B. 2003. SCARECROW is involved in positioning the stem cell niche in the Arabidopsis root meristem. *Genes & Development* **17**: 354–358.

Samalova M, Brzobohaty B, Moore I. 2005. pOp6/LhGR: a stringently regulated and highly responsive dexamethasone-inducible gene expression system for tobacco. *The Plant Journal* **41**: 919–935.

Schindele A, Gehrke F, Schmidt C, Röhrig S, Dorn A, Puchta H. 2022. Using CRISPR-Kill for organ specific cell elimination by cleavage of tandem repeats. *Nature Communications* **13**: 1502.

Schürholz A-K, López-Salmerón V, Li Z, Forner J, Wenzl C, Gaillochet C, Augustin S, Barro AV, Fuchs M, Gebert M *et al.* 2018. A comprehensive toolkit for inducible, cell type-specific gene expression in Arabidopsis. *Plant Physiology* **178**: 40–53.

Sharma A, Pervaiz ZH, Wysocka-Diller J. 2022. SCR suppressor mutants: role in hypocotyl gravitropism and root growth in *Arabidopsis thaliana*. *International Journal of Plant Biology* **13**: 506–522.

Sozzani R, Cui H, Moreno-Risueno MA, Busch W, van Norman JM, Vernoux T, Brady SM, Dewitte W, Murray JAH, Benfey PN. 2010. Spatiotemporal regulation of cell-cycle genes by SHORTROOT links patterning and growth. *Nature* **466**: 128–132.

Steinert J, Schiml S, Fauser F, Puchta H. 2015. Highly efficient heritable plant genome engineering using Cas9 orthologues from *Streptococcus thermophilus* and *Staphylococcus aureus*. *The Plant Journal* **84**: 1295–1305.

Tsugeki R, Fedoroff NV. 1999. Genetic ablation of root cap cells in Arabidopsis. *Proceedings of the National Academy of Sciences, USA* **96**: 12941–12946.

Weijers D, van Hamburg J-P, van Rijn E, Hooykaas PJJ, Offringa R. 2003. Diphtheria toxin-mediated cell ablation reveals interregional communication during Arabidopsis seed development. *Plant Physiology* **133**: 1882–1892.

Wysocka-Diller JW, Helariutta Y, Fukaki H, Malamy JE, Benfey PN. 2000. Molecular analysis of SCARECROW function reveals a radial patterning mechanism common to root and shoot. *Development* **127**: 595–603.

Supporting Information

Additional Supporting Information may be found online in the Supporting Information section at the end of the article.

Fig. S1 Boxplots for the Dex-induced CRISPR-Kill activity for lateral root elimination.

Fig. S2 Boxplots for the inducible CRISPR-Kill system for root stem cell ablation.

Fig. S3 Boxplots for the Dex-induced CRISPR-Kill system with a multi-tissue promotor in the RAM.

Table S1 Determination of the sgRNA expression via quantitative real-time PCR.

Table S2 Source data for the determination of the relative survival rate.

Table S3 Dex-induced CRISPR-Kill system with a multi-tissue promotor in the SAM.

Table S4 Source data for the Dex-induced CRISPR-Kill activity for lateral root elimination.

Table S5 Source data for the inducible CRISPR-Kill system for root stem cell ablation.

Table S6 Source data for the Dex-induced CRISPR-Kill system with a multi-tissue promotor in the RAM.

Please note: Wiley is not responsible for the content or functionality of any Supporting Information supplied by the authors. Any queries (other than missing material) should be directed to the *New Phytologist* Central Office.